Nonlinear interaction of transverse modes in a CO_2 laser

R. López-Ruiz, G. B. Mindlin, and C. Pérez-García

Departamento de Física y Matemática Aplicada, Universidad de Navarra, E-31080 Pamplona, Navarra, Spain

J. R. Tredicce

Institute Non Lineaire de Nice, F-06034, Nice Cedex, France

We show the possibility of achieving experimentally a Takens-Bogdanov bifurcation for the nonlinear interaction of two transverse modes ($l = \pm 1$) in a CO_2 laser. The system has a basic O(2) symmetry which is perturbed by some symmetry-breaking effects that still preserve the Z_2 symmetry. The pattern dynamics near this codimension-two bifurcation under such symmetries is described. This dynamics changes drastically when the laser properties are modified.

I. INTRODUCTION

Pattern formation in physical systems is an area of active research. It has been recently pointed out that lasers can provide a "test bench" for these studies, as it is possible to have many active transverse modes which, through nonlinear interaction, give a complicated spatiotemporal dynamics [1]. Recent evidence shows that some interesting phenomena such as defects, vortices, chaotic alternancy, etc., can be found in laser systems [2]. Unfortunately, in most cases these works do not enlighten the mechanisms behind the transition from simple solutions to the spatiotemporal uncorrelated ones. A step in understanding this complex dynamics is to study the nonlinear interaction among a few modes which bifurcate from the zero solution [3,4]. This paper strives in this direction.

It has been reported that some qualitative features of the transverse patterns of intensity observed in CO_2 lasers can be explained in the frame of the theory of bifurcations in the presence of symmetries [1,5]. The laser tube imposes the O(2) symmetry (rotations and reflections). The mode amplitude equations having this symmetry predict that the stable modes with nonzero angular momentum bifurcating from zero should be traveling waves, in contradiction with experiments. Anisotropies in the laser parameters (pumping, losses, or disalignments in the setup, etc.) break the O(2) symmetry. An agreement between theory and experiment can be reached by introducing a symmetry-breaking term preserving the Z_2 symmetry. This model successfully predicts the stability of the standing waves widely observed in the laser transverse section. The prediction of secondary solutions that arise from the standing waves is another achievement of the model with "imperfect" symmetry. These solutions are either a mixture of a standing wave and traveling waves, or modulated waves that appear from a Hopf bifurcation of the standing waves.

The conditions for a CO_2 laser displaying those solutions that bifurcate simultaneously from the standing wave (codimension-two point) are analyzed here. The dynamics near such bifurcation and the intensity patterns resulting from this situation are investigated. Work in this direction has been done in traveling-wave convection in binary mixtures. In this case, the presence of distant sidewalls in systems that are translation-invariant break the O(2) symmetry and the simplest possible symmetry-breaking effects are discussed when the system undergoes a Hopf bifurcation [6].

This paper is organized as follows. In Sec. II we discuss the properties of the physical system and we present the equations describing the dynamics of the active primary modes in this system. A linear study of these modes is performed in order to identify the possible secondary solutions that might bifurcate from them. In Sec. III we analyze the conditions under which a nonlinear interaction between the secondary solutions is possible, and a normal form reduction of the equations is carried out. After computing the coefficients of this normal form in terms of parameter values for a CO_2 laser, we determine the two possible scenarios. We discuss the kind of patterns that could be observed under these conditions in Sec. IV. Section V sets out some conclusions and provides some guidelines for further experimental observation.

II. MODEL AND PRIMARY BIFURCATIONS

The physical system is a CO_2 laser in a Fabry-Pérot cavity. The active medium is contained in a cylindrical tube, with a perfectly reflecting plane mirror at one end and a curved mirror with partial reflectivity at the other end. Physically, the effective curvature of this mirror can be modified by inserting a passive optical device. Moreover, we are interested in the interaction among modes with nonzero angular momentum. This can only be achieved experimentally by placing an intracavity iris which inhibits the Gaussian mode [1].

We therefore consider that the electric field can be expressed in terms of the modes arising from a Hopf bifurcation from the zero solution,

$$E = P_1(r)L_1(z)e^{i\omega t}(z_1 e^{il\theta} + z_2 e^{-il\theta}) , \qquad (1)$$

where $P_1(r)$ and $L_1(z)$ account for the radial and longitudinal dependence of the bifurcating modes, respectively, and θ is the angular variable. The integer l denotes the angular momentum and ω is the temporal frequency of the modes. The complex amplitudes z_1 and z_2 are governed by the equations

$$z_1' = \lambda z_1 - A(z_1 z_1^* + 2 z_2 z_2^*) z_1 + \epsilon z_2 , \tag{2}$$

$$z_2' = \lambda z_2 - A(2 z_1 z_1^* + z_2 z_2^*) z_2 + \epsilon z_1 , \tag{3}$$

which are obtained by substituting the electric field E into the Maxwell-Bloch equations and truncating to third order [7]. The complex coefficients λ and A can be expressed in terms of the atomic inversion and decay rates, the detuning, and a convolution between the pumping profile and the spatial part of the modes. (The explicit form of these coefficients can be found in the Appendix). Note that the complex parameter ϵ (which carries information about the asymmetries in the laser parameters, such as anisotropies in the pumping or in the Brewster windows [4]) accounts for the breaking of the O(2) symmetry (see Appendix). As the equations remain invariant under the operation $z_1 \leftrightarrow z_2$, they preserve a Z_2 symmetry.

We substitute $z_i = \rho_i e^{i\phi_i}$, $\epsilon = \rho_\epsilon e^{i\phi_\epsilon}$, and $\lambda = \mu + i\Omega_1$ in Eqs. (2) and (3). After scaling by $A^r = \text{Re}(A)$ we arrive at the following system:

$$\rho_1' = \mu \rho_1 - (\rho_1^2 + 2\rho_2^2)\rho_1 + \rho_\epsilon \rho_2 \cos(\delta + \phi_\epsilon) , \tag{4}$$

$$\rho_2' = \mu \rho_2 - (2\rho_1^2 + \rho_2^2)\rho_2 + \rho_\epsilon \rho_1 \cos(\delta - \phi_\epsilon) , \tag{5}$$

$$\delta' = \alpha(\rho_1^2 - \rho_2^2) - \rho_\epsilon[\rho_1/\rho_2 \sin(\delta - \phi_\epsilon) + \rho_2/\rho_1 \sin(\delta + \phi_\epsilon)] , \tag{6}$$

and a fourth equation for the evolution of the phase ϕ_1, which is uncoupled from these three equations. The variable $\delta = \phi_2 - \phi_1$ is the phase difference between the two modes. Notice that its dynamic is nontrivial because the broken-symmetry term couples this phase difference with the mode amplitudes. (For simplicity, we use the same notation for the rescaled parameters). The information about the curvature, detuning, etc., contained in A^r remains in the coefficient $\alpha = A^i / A^r$.

The primary bifurcations from zero in equations (4)–(6) are four stationary solutions: two standing waves SW_0 ($\rho_1 = \rho_2, \delta = 0$), SW_π ($\rho_1 = \rho_2, \delta = \pi$) and two solutions, which are a mixture between traveling waves and standing waves TW_1 ($\rho_1 > \rho_2, \delta > 0$), TW_2 ($\rho_1 < \rho_2, \delta < 0$). These solutions give four stationary patterns their stability depending on the parameter settings. By an appropriate selection of the parameters in this situation a good qualitative agreement with a previous experiment has been obtained [3].

III. TAKENS-BOGDANOV BIFURCATION

In this paper the attention is focused in investigating the secondary bifurcations from the standing wave and on the new dynamics arising from the nonlinear interaction between those secondary solutions. Before proceed-
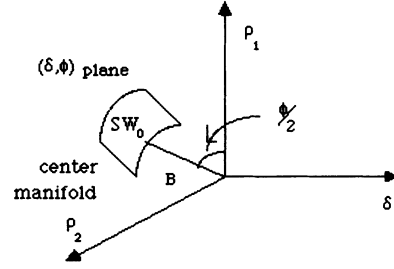

FIG. 1. Sketch of the change of variables (7) performed in Eqs. (4)–(6). In these variables the dynamics of interest takes place near the (δ, ϕ) plane (center manifold).

ing with the stability analysis it is convenient to perform the following change of variables:

$$\rho_1 = B \cos(\phi/2), \quad \rho_2 = B \sin(\phi/2) , \tag{7}$$

because the B direction is decoupled from the (ϕ, δ) plane in this representation (Fig. 1). The standing-wave solutions are simply $SW_{0,\pi}$:

$$B_{0,\pi}^2 = 2\frac{\mu \pm \rho_\epsilon \cos\phi_\epsilon}{3}, \quad \phi_{0,\pi} = \pi/2, \quad \delta_{0,\pi} = 0, \pi .$$

A linear stability analysis around these solutions leads to the following eigenvalues. In the B direction the eigenvalue is simply $-2[\mu \pm \rho_\epsilon \cos(\phi_\epsilon)]$, where the $\pm$ correspond to the $SW_{0,\pi}$ solutions, respectively. The eigenvalues corresponding to the (ϕ, δ) plane are obtained from the following matrix:

$$\begin{bmatrix} \frac{2}{3}\mu \mp \frac{4}{3}\rho_\epsilon \cos\phi_\epsilon & \pm 2\rho_\epsilon \sin\phi_\epsilon \\ \frac{2\alpha}{3}(\mu \pm \rho_\epsilon \cos\phi_\epsilon) \mp 2\rho_\epsilon \sin\phi_\epsilon & \mp 2\rho_\epsilon \cos\phi_\epsilon \end{bmatrix} . \tag{8}$$

Now we determine the conditions for the appearance of a codimension-two (CT) point.

A. Codimension-two point

The codimension of a bifurcation is the smallest dimension of a parameter space which contains the bifurcation in a persistent way. In our case, the CT point is determined by a degenerated double zero eigenvalue in the matrix (8). This results from the interaction between a Pitchfork bifurcation and a Hopf bifurcation. [The Pitchfork bifurcation gives rise to two new solutions ($TW_{1,2}'$). The solution resulting form the Hopf bifurcation is the so-called modulated wave (MW).] This CT point is obtained when the parameters verify

$$\mu = \pm 5\rho_\epsilon \cos\phi_\epsilon , \tag{9}$$

$$\alpha^{-1} = -\tan(2\phi_\epsilon) . \tag{10}$$

For a given α, and as $\mu > 0$ (the two modes were born supercritically), these relations (9) and (10) lead to four solutions as sketched in Fig. 2. Solutions I and IV are associated with the SW_0 [plus sign in Eq. (9)]: (I $\equiv \phi_\epsilon^0$; IV $\equiv \phi_\epsilon^0 + 3\pi/2$), while II and III (II $\equiv \phi_\epsilon^0 + \pi/2$; III $\equiv \phi_\epsilon^0 + \pi$) correspond to SW_π [minus sign in Eq. (9)].
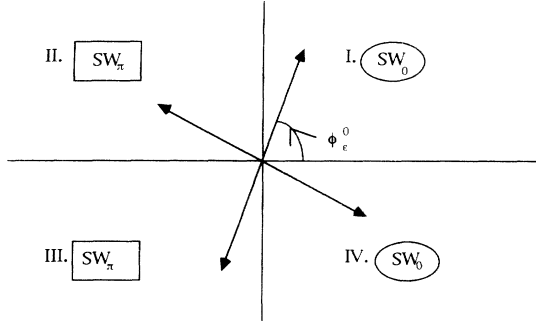
FIG. 2. The four possible solutions of the equation system (9) and (10) (under the condition $\mu > 0$), where a Takens-Bogdanov bifurcation takes place. They are shown in the angular ϕ_ϵ space. The dynamics around all of them is equivalent.

As Eqs. (4)–(6) are invariant under the transformation $(\phi_\epsilon; \rho_1(t), \rho_2(t), \delta(t)) \rightarrow (\phi_\epsilon + \pi; \rho_1(t), \rho_2(t), \delta(t) + \pi)$ (Z_2 − residual symmetry), the local dynamics around I and III is equivalent. The same argument can be applied to solutions II and IV.

For the sake of simplicity, we analyze only the local behavior around instability I (and IV) in Sec. III B. [Calculations for cases II (and III) follow the same procedure.]

B. Normal form reduction

Let us recall some general features of a dynamical system linearized around a stationary solution. When some eigenvalues have zero real part, the flow near this fixed point can be quite complicated. The linear space spanned by the states corresponding to this null real part eigenvalues is known as *center eigenspace*. The invariant manifold tangent to the center eigenspace constitutes the *center manifold*. The local dynamics "transverse" to this manifold is relatively simple, since it is controlled by the "fast" variables of the flow. The asymptotic behavior of the flow develops on the center manifold. The family of these behaviors that arise in the vicinity of this fixed point when the parameters are slightly varied is called the *unfolding* of the bifurcation. The "simplest" set of equations that reproduces generically all these behaviors is called the *normal form* of the bifurcation.

The unfolding of the bifurcation for solution I (dynamics near SW_0) is described by the normal form

$$x' = y ,\tag{11}$$

$$y' = ax + by \mp x^3 - x^2 y ,\tag{12}$$

which was first studied by Takens and Bogdanov (TB) [8,9]. It can show in fact two different behaviors depending on the choice of the sign $\mp$.

Now we show that Eqs. (4)–(6) reduce to Eqs. (11) and (12) around SW_0 if the conditions (9) and (10) for solution I hold. Let us note that in this case $\phi_\epsilon^0 \in (0, \pi/2)$ for any given α [Eqs. (9) and (10)]. We perform a last change of variables: $(B, \phi, \delta) \rightarrow (B, u, \delta)$ with $u = (\rho_2^2 - \rho_1^2)/B^2$ $= -\cos\phi$. The equations can be rewritten as follows:

$$B' = \mu B - \tfrac{1}{2}(3 - u^2)B^3 + \rho_\epsilon B(1 - u^2)^{1/2} \cos\phi_\epsilon \cos\delta ,\tag{13}$$

$$u' = u(1 - u^2)B^2 + 2\rho_\epsilon(1 - u^2)^{1/2}(\sin\phi_\epsilon \sin\delta - u \cos\phi_\epsilon \cos\delta) ,\tag{14}$$

$$\delta' = \alpha B^2 u - \frac{2\rho_\epsilon}{\sqrt{1 - u^2}}(\cos\phi_\epsilon \sin\delta + u \sin\phi_\epsilon \cos\delta) .\tag{15}$$

To obtain the unfolding of the bifurcation we consider, for small variations of the parameters,

$$\phi_\epsilon = \phi_\epsilon^0 + \beta, \quad \frac{\mu}{\rho_\epsilon} = 5 \cos\phi_\epsilon^0 + q .$$

The fast variable B is "enslaved" by the other two variables and can be adiabatically eliminated after assuming $B' = 0$. Then the central manifold is two-dimensional and can be expressed as a function of (u, δ). As usual in a local stability analysis, we will keep up to third-order terms. To obtain the normal form [Eqs. (11) and (12)], the following change of variables $(u, \delta) \rightarrow (x = \tfrac{1}{2}(u/\tan(\phi_\epsilon^0) - \delta), y = \tfrac{1}{2}(u/\tan(\phi_\epsilon^0) + \delta))$ is introduced. This allows us to obtain the right linear part of the normal form. We can rearrange the equations by means of another near-identity change on the new variables (x, y). After these changes the normal form of the bifurcation reads as

$$x' = y ,\tag{16}$$

$$y' = \mu_1 x + \mu_2 y + Cx^3 + Dx^2 y ,\tag{17}$$

where

$$\mu_1 = \frac{4}{3}\left[\frac{1 + \alpha \tan(\phi_\epsilon^0)}{\cos(\phi_\epsilon^0)}q - \frac{\alpha \tan^3(\phi_\epsilon^0) + 8\alpha \tan(\phi_\epsilon^0) + 7}{\tan(\phi_\epsilon^0)}\beta \right] ,\tag{18}$$

$$\mu_2 = \frac{2}{3}\left[\frac{1}{\cos(\phi_\epsilon^0)}q + 5 \tan^2(\phi_\epsilon^0)\beta \right] ,\tag{19}$$

$$C = \frac{2}{3}[2 - \alpha \tan(\phi_\epsilon^0) - 3\alpha\tan^3(\phi_\epsilon^0)] ,\tag{20}$$

$$D = \frac{-1}{6}[80\alpha \tan(\phi_\epsilon^0) + 32] ,\tag{21}$$

$$\alpha = \frac{\tan^2(\phi_\epsilon^0) - 1}{2 \tan(\phi_\epsilon^0)} .\tag{22}$$

Notice that the coefficients in this normal form mainly depend on the value of α. As D is always negative the unfolding of the bifurcation depends mainly on C, which is a function mainly of α. The unfolding is qualitatively different when C changes from negative to positive, i.e., for the conditions

$$C = 0 \Longrightarrow \tan(\phi_\epsilon^*) = (5/3)^{1/2} \Longrightarrow \alpha_* = -\text{cotan}(2\phi_\epsilon^*) = 0.258 .\tag{23}$$
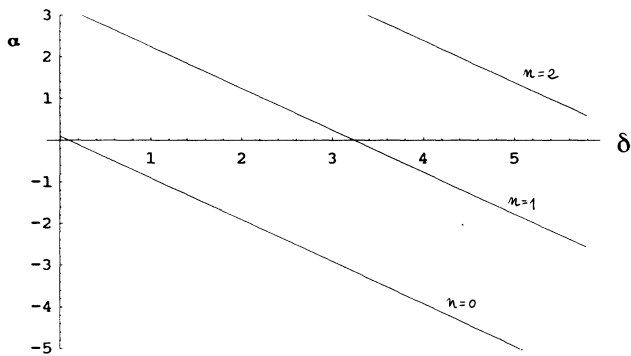
(The unfoldings corresponding to $C > 0$ and $C < 0$ will be described in detail in Sec. IV.) In the Appendix, the dependence of α on the laser properties is calculated for different transverse modes. This calculation shows that the transition point [Eq. (23)] can be reached in a CO_2 laser (Fig. 3).
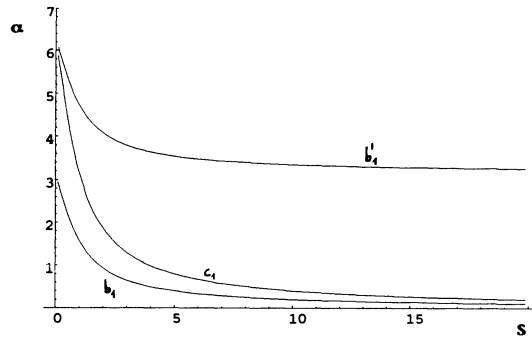

(a)
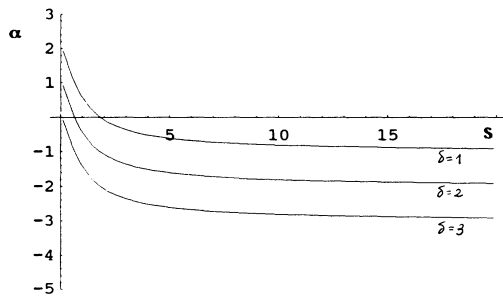
(b)

(c)

FIG. 3. (a) Plot of the value of α as the curvature s of the cavity is varied for three different modes: $b_1 = (2,1,0)$; $c_1 = (4,1,0)$; and $b'_1 = (2,1,1)$. The detuning δ is fixed: $\delta = 0$. (b) Plot of α on s for the mode $b_1 = (2,1,0)$, when the detuning takes the values $\delta = 1$, $\delta = 2$, and $\delta = 3$. (c) Plot of α on δ for three modes with different longitudinal behavior: $b_1 = (2,1,0)$, $b'_1 = (2,1,1)$, and $b''_1 = (2,1,2)$. (The curvature is fixed: $s = 20$.) The transition explained in relation (23) is obtained for $\alpha = 0.258$. (See Appendix for the notation.)

IV. PATTERN DYNAMICS IN THE NEIGHBORHOOD OF THE BIFURCATION

In Sec. III we obtained the conditions for the two possible kinds of TB bifurcation that can take place in the transverse section of a CO_2 laser. Depending on the sign of parameter C, two qualitatively different scenarios are possible. Now we describe the two different dynamics in some detail,

$$\alpha \in (-\infty, 0.258) \equiv \phi_\epsilon \in (0, 0.912) \ .$$

This corresponds to the case $C > 0$ ($D < 0$). The unfolding near the bifurcation is presented in Fig. 4(a). From this unfolding the following general features are read. First, the solutions SW_0 (Fig. 5) as well as the two TW' (created after a Pitchfork bifurcation from the SW_0) are unstable for nearly all the parameter space. The sys-
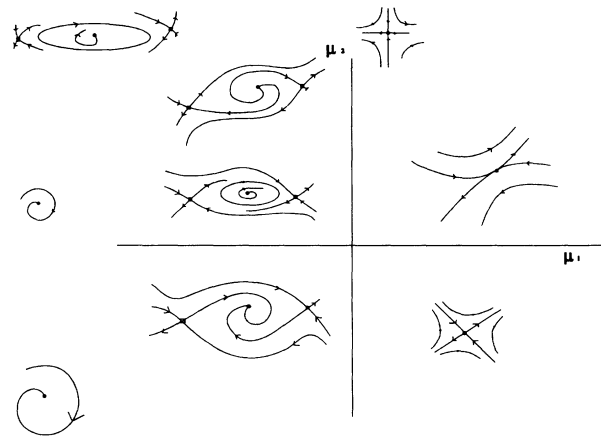
(a)
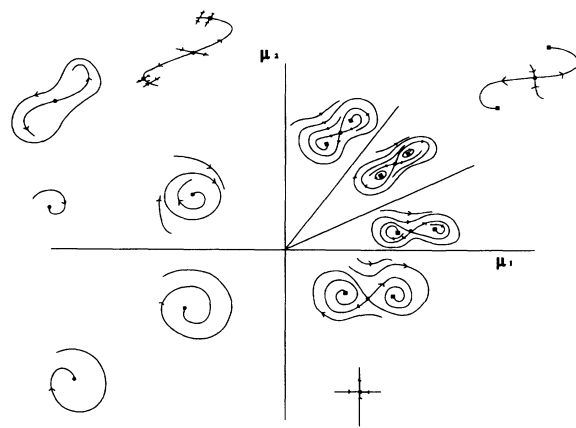
(b)

FIG. 4. Unfolding diagrams for the two kinds of Takens-Bogdanov bifurcation [see the normal form (16) and (17)] that can be achieved: squares $\equiv TW'_{1,2}$ (or $TW_{1,2}$); circles $\equiv SW_0$. The outer figures of the diagram are obtained simulating the total number of equations (4)–(6) far from the instability. (a) For $\alpha < 0.258$, where $C > 0, D < 0$. (b) For $\alpha > 0.258$ where $C < 0, D < 0$.
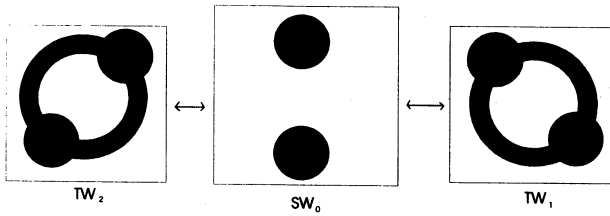
FIG. 5. Patterns that can be observed: TW_1 (or TW_1' if it is close to SW_0); SW_0; and TW_2 (or TW_2'). The arrows represent the periodic alternancy $TW_1' \leftrightarrow SW_0 \leftrightarrow TW_2'$ that takes place for $C < 0$. Also possible is another periodic alternancy $TW_1' \leftrightarrow TW_2'$ or $TW_1 \leftrightarrow TW_2$ for $C > 0$.

tem almost always evolves to some of the traveling solutions, $TW_1 \equiv (\rho_1, \rho_2, \delta)$ or $TW_2 \equiv (\rho_2, \rho_1, -\delta)$. So, one of the conjugate patterns in Fig. 5 would be observed when we tune the parameter values around the bifurcation point. Second, the analysis of the full equations (4)–(6) shows that far away from the bifurcation point a limit cycle appears as a global bifurcation from a heteroclinic connection between these patterns $(TW_{1,2})$. This solution will look like a periodic alternancy between the two $TW_{1,2}$ due to the critical slowing down that takes place in the neighborhood of these points (Fig. 5).

$$\alpha \in (0.258, \infty) \equiv \phi_\epsilon \in \left[0.912, \frac{\pi}{2} \right] :$$

In this case $C < 0$ ($D < 0$) and there is a strong change in the pattern evolution [Fig. 4(b)]. Near the bifurcation point the SW_0, weak oscillations $TW_{1,2}' \leftrightarrow SW_0$ (quasistationary patterns), or a periodic alternancy $TW_1' \leftrightarrow SW_0 \leftrightarrow TW_2'$ will be observed. The latter corresponds to a limit cycle that grows in a global bifurcation from a homoclinic connection of the SW_0. When we go far away in the parameter space a periodic alternancy between the two $TW_{1,2}$ is found again.

Notice that the frequency associated to the oscillation between the patterns (Hopf bifurcation from SW_0) is of order $\omega_{osc}^2 \sim |\mu_1| \sim \rho_\epsilon |q|$. So it is much slower than the temporal scale associated to the modes.

V. CONCLUSIONS

In this article, a model for the evolution of transverse modes $(l = \pm 1)$ in a CO_2 laser has been studied. Due to the unavoidable anisotropies in the laser setup, some terms that break the natural $O(2)$ symmetry must be included. This model is quite successful in predicting the stability of the primary solutions SW found in recent experiments. The possible secondary solutions have been determined.

The symmetry breaking term allows the possibility of a codimension-two point bifurcating from the SW. This point appears when secondary solutions from a Pitchfork and a Hopf bifurcation interact simultaneously at the same point (Takens-Bogdanov bifurcation). A normal form reduction procedure allowed us to capture the main dynamical properties of the system near that bifurcation.

The calculations of the normal form coefficients for different realistic values in a CO_2 laser showed that two possible dynamical scenarios are possible.

The intensity patterns that correspond to the dynamical interaction between these modes $(l = \pm 1)$ have been described for these two scenarios. Near the bifurcation one can get stationary patterns (standing waves SW or traveling waves TW) or oscillations between the SW and the new conjugate patterns TW'. Far away from the point bifurcation a global bifurcation of a heteroclinic connection leads to a periodic alternancy between TW patterns. These patterns look quasistationary due to a critical slowing down near the TW solutions.

Remarkably, this "rich" dynamics cannot be observed without a symmetry-breaking term. It is important to stress that the interpretation of complicated pattern dynamics beyond the particular problem studied here could lie on simple symmetry considerations.

APPENDIX

It is clear that the analysis presented in this work strongly relies on the terms multiplying ϵ in Eqs. (2) and (3). An asymmetry in the pumping profile gives rise to this linear coupling between the equations for the mode amplitudes z_1 and z_2. The dependence of ϵ in terms of laser parameters was derived in Ref. [4]. The result was

$$\epsilon = \frac{K_\epsilon}{\beta - i\Omega_1}, \tag{A1}$$

where K_ϵ is the parameter governing the asymmetry in the pumping profile $[K_{pumping} = K(r) + 2K_\epsilon \cos(2\theta)]$, β is the rate of decay of the atomic polarization, and Ω_1 is the slow temporal frequency of the empty cavity mode.

In the following, we compute the value of $\alpha = A^i / A^r$ for the primary bifurcating modes with angular momentum $l = \pm 1$. It is shown that the transition point $\alpha = 0.258$ between the two possible TB bifurcations can be obtained in a CO_2 laser.

The spatial coordinates of the problem are (r, θ, z), where (r, θ) corresponds to the transversal section of the cavity and z to the longitudinal direction $(z \in [-L, 0])$. The new coordinates (ξ, θ, z) are introduced [7]:

$$\xi^2 = \left[\frac{r}{L} \right]^2 ks(s^2 + z^2)^{-1}, \tag{A2}$$

$$s = \left[\frac{2R_m}{L} - 1 \right]^{1/2}, \tag{A3}$$

where s is the effective curvature, L ($\sim 1m$) the cavity length, R_m the curvature radius of the spherical mirror

and $k = 2\pi L / \lambda$ is the wave number.

The field is expanded (following [7]) in terms of empty cavity modes,

$$\begin{bmatrix} \Phi^+ \\ \Phi^- \end{bmatrix} = \sum z_\mu \begin{bmatrix} a_\mu^+ \\ a_\mu^- \end{bmatrix} . \quad (A4)$$

This expansion is introduced in the Maxwell-Bloch equations (a brief review is done in [4]), and projected on each mode. The temporal evolution for the cavity mode amplitudes z_α is then

$$z_\alpha' = \lambda_\alpha z_\alpha + M_{\alpha\mu\nu\beta} z_\mu z_\nu^* z_\beta + \text{h.o.t.} , \quad (A5)$$

where the expressions of the coefficients $\lambda_\alpha, M_{\alpha\mu\nu\beta}$ are given in [7] and h.o.t. denotes higher-order terms.

The mode $a_\mu = (a_\mu^+, a_\mu^-)$ has the functional form

$$a_\mu = (R_\mu(\xi) e^{-i\phi_\mu} e^{il_\mu\theta}, R_\mu(\xi) e^{i\phi_\mu} e^{+il_\mu\theta}) . \quad (A6)$$

The coefficient ϕ_{mu} is given by

$$\phi_\mu = \Omega_\mu z - p_\mu \tan\left[\frac{z}{s} \right] , \quad (A7)$$

with

$$\Omega_\mu = n_\mu \pi + p_\mu \arctan\left[\frac{1}{s} \right] - \delta , \quad (A8)$$

where (p_μ, l_μ, n_μ) are three integers that characterize the mode; $p_\mu = 2n_r + l_\mu + 1$ is essentially the total transverse energy of the laser beam (n_r is the radial quantum number), l_μ is the angular momentum around the z axis, and n_μ is associated to the longitudinal behavior of the mode. $R_\mu(\xi)$ is the radial dependence and $\delta = k \bmod 2\pi$ is the detuning of the cavity. Making the operations indicated in [7], we obtain the general form,

$$\lambda_\alpha = \left[-\chi + \frac{\bar{K}\beta}{\beta^2 + \Omega_\alpha^2} \right] - i\Omega_\alpha \left[1 - \frac{\bar{K}}{\beta^2 + \Omega_\alpha^2} \right] , \quad (A9)$$

$$M_{\alpha\mu\nu\beta} = F(\Omega_\mu, \Omega_\nu, \Omega_\beta) \frac{L^2}{ks} \int \int \int K(\xi) R_\alpha(\xi) R_\nu(\xi)$$
$$\times R_\mu(\xi) R_\beta(\xi)$$
$$\times [4\cos(\phi_\alpha + \phi_\nu - \phi_\mu - \phi_\beta)$$
$$+ 2\cos(\phi_\alpha - \phi_\nu - \phi_\mu + \phi_\beta)] \xi \, d\xi \, dz \, d\theta ,$$

$$(A10)$$

where the pumping profile $K(\xi) = \bar{K}$ is considered constant along the whole beam width and χ gives account for the cavity losses.

After applying these procedures to our two mode interaction model,

$$z_1' = \lambda z_1 - A(z_1 z_1^* + 2z_2 z_2^*) z_1 + \epsilon z_1 , \quad (A11)$$

$$z_2' = \lambda z_2 - A(2z_1 z_1^* + z_2 z_2^*) z_2 + \epsilon z_2 , \quad (A12)$$

we can identify $A = -M_{1111}$, which, according to expression (A8), gives

$$A = -M_{1111} = \text{const} \times \frac{2\beta}{\beta^2 + \Omega_1^2} \frac{1}{\beta - i\Omega_1} \int 6[R_1(\xi)]^4 \xi \, d\xi .$$

$$(A13)$$

These calculations have been performed for the primary bifurcating modes $a_\mu = (p, l, n)$:

$$b_1 \equiv (2, 1, 0) \rightarrow R_1^2(\xi) \sim \xi^2 e^{-\xi^2} , \quad (A14)$$

$$c_1 \equiv (4, 1, 0) \rightarrow R_1^2(\xi) \sim (2 - \xi^2)^2 \xi^2 e^{-\xi^2} , \quad (A15)$$

$$b_1' \equiv (2, 1, 1) \rightarrow R_1^2(\xi) \sim \xi^2 e^{-\xi^2} . \quad (A16)$$

In general, the coefficient $\alpha = A^i / A^r$ depends on the cavity curvature s and on the detuning δ. We plot the dependency of α on s and δ for the primary modes in Fig. 3. α decreases when the curvature (or detuning) increases and the transition value $\alpha = 0.258$ can be reached for a sufficiently high curvature s.

[1] C. Green, G. B. Mindlin, E. D'Angelo, H. G. Solari, and J. R. Tredicce, Phys. Rev. Lett. **65**, 3124 (1990).

[2] F. T. Arecchi, G. Giacomelli, P. L. Ramazza, and S. Residori, Phys. Rev. Lett. **67**, 3749 (1991).

[3] E. D'Angelo, E. Izaguirre, G. B. Mindlin, G. Huyet, L. Gil, and J. R. Tredicce, Phys. Rev. Lett. **68**, 3702 (1992).

[4] R. López-Ruiz, G. B. Mindlin, C. Pérez-García, and J. R. Tredicce, Phys. Rev. A **47**, 500 (1993).

[5] M. Golubitsky, I. Stewart, and D. Schaeffer, *Singularities and Groups in Bifurcation Theory*, Applied Mathematical Sciences Vol. 69 (Springer-Verlag, New York, 1988).

[6] G. Dangelmayr, M. Wegelin, and E. Knobloch, Eur. J. Mech. B **10**, 125 (1991).

[7] H. Solari and R. Gilmore, J. Opt. Soc. Am. B **7**, 828 (1990).

[8] J. Guckenheimer and P. Holmes, *Nonlinear Oscillations, Dynamical Systems and Bifurcation of Vector Fields*, Applied Mathematical Sciences Vol. 42 (Springer-Verlag, New York, 1983).

[9] G. Dangelmayr and E. Knobloch, Nonlinearity **4**, 399 (1991).